Journal of Functional Foods 62 (2019) 103546

Contents lists available at ScienceDirect

Journal of Functional Foods

journal homepage: www.elsevier.com/locate/jff

Resveratrol-enriched grape seed oil (*Vitis vinifera* L.) protects from white fat dysfunction in obese mice

Mohammed Mahanna[a], Maria C. Millan-Linares[b], Elena Grao-Cruces[a], Carmen Claro[c], Rocío Toscano[a,d], Noelia M. Rodriguez-Martin[a,d], Maria C. Naranjo[e], Sergio Montserrat-de la Paz[a,*]

[a] Department of Medical Biochemistry, Molecular Biology, and Immunology, School of Medicine, Universidad de Sevilla, Av. Dr. Fedriani 3, 41009 Seville, Spain
[b] Cell Biology Unit, Instituto de la Grasa, CSIC, Ctra. de Utrera Km. 1, 41013 Seville, Spain
[c] Department of Pharmacology, Pediatrics, and Radiology, School of Medicine, Universidad de Sevilla, Av. Dr. Fedriani 3, 41071 Seville, Spain
[d] Department of Food & Health, Instituto de la Grasa, CSIC, Ctra. de Utrera Km. 1, 41013 Seville, Spain
[e] Department of Food Technology, Universitat de Lleida, Av. Alcalde Rovira Roure 191, 25198 Lleida, Spain

ARTICLE INFO

Keywords:
Resveratrol
Grape seed oil
Phenolic compounds
Obesity
Adipose tissue

ABSTRACT

Grape skin and seed oil are winemaking by-products with a potential nutraceutical value. This study aimed to evaluate the effects of resveratrol-enriched grape seed oil (GSO) administration on white adipose tissue (WAT) dysfunction in obese mice. Male mice were divided into four groups (n = 10/group): the chow diet (CD) group; the high-fat diet (HFD) group was fed fat from milk cream (rich in saturated fatty acids), and the HFD-GSO and HFD-GSO + R groups were fed fat from GSO in absence or presence of resveratrol (200 mg/kg/day), respectively. Glucose tolerance, metabolic profile, and inflammatory cytokines were determined. Histological studies were carried out in WAT and brown AT, RT-qPCR and western blot were used to determine the gene and protein expression. In the setting of obesity, our results unveil a novel nutritional value for winemaking by-products by which resveratrol-enriched GSO from *Vitis vinifera* L. in obesogenic diets favor WAT and immunometabolic homeostasis.

1. Introduction

The global prevalence of obesity has increased rapidly in recent years, and the number of overweight or obese adults worldwide is expected to reach 3.3 billion by 2030 (Gonzalez-Muniesa et al., 2017). In addition to genetic mechanisms, the continuous and excessive exposure to energy-dense foods paired with a sedentary lifestyle has driven the obesity pandemic (Stelmach-Mardas et al., 2016). White adipose tissue (WAT) is the primary site for energy storage and a dynamic endocrine organ secreting a range of bioactive molecules (adipokines, lipokines, and extracellular vesicles) to communicate with other cell types, thereby exerting diverse local and systemic effects with a major relevance on whole-body homeostasis (Choe, Huh, Hwang, Kim, & Kim, 2016). Upon exceeding its expansion capacity by an enlargement in the size of adipocytes (hypertrophy), an increase in the number of adipocytes (hyperplasia) or both, WAT becomes dysfunctional and promotes the recruitment of immune cells, which ultimately leads to a low-grade inflammatory state (Macdougall & Longhi, 2019). Self-sustained lipolysis orchestrates the accumulation of monocyte-derived macrophages in the obese WAT (Guo et al., 2015), where they polarize or switch from an M2 anti-inflammatory phenotype towards an M1 pro-inflammatory phenotype (Zhao et al., 2018).

Grape, the berries of *Vitis vinifera* L., is one of the most economically important plant species due to its diverse uses in production of wine, grape juice and other food products (Ding et al., 2018). During wine production, approximately 25% (w/w) of the grape results in by-products, which are comprised of skins and seeds (Millan-Linares et al., 2018). Resveratrol (3,5,4′- trihydroxystilbene), is a stilbenoid poly-

Abbreviations: BAT, brown adipose tissue; CD, chow diet; GSO, grape seed oil; HFD, high-fat diet; IL, interleukin; OGTT, oral glucose tolerance test; SFA, saturated fatty acid; TNF, tumor necrosis factor; UCP, uncoupling protein; WAT, white adipose tissue

* Corresponding author.
E-mail address: delapaz@us.es (S. Montserrat-de la Paz).

https://doi.org/10.1016/j.jff.2019.103546
Received 17 June 2019; Received in revised form 22 August 2019; Accepted 27 August 2019

phenol which is naturally present in the skin and seeds of grapes (Yang, Xu, Qian, & Xiao, 2017). However, resveratrol is not detected in grape seed oil (GSO) (Millan-Linares et al., 2018). Clinical trials and animal experiments have shown that resveratrol has numbers of health benefits, including the prevention of cancer (Ko et al., 2017), aging (Diaz, Degens, Vanhees, Austin, & Azzawi, 2016), obesity (Aguirre, Fernandez-Quintela, Arias, & Portillo, 2014), diabetes mellitus (Szkudelski & Szkudelska, 2015), and cardiovascular disease (Bonnefont-Rousselot, 2016). Anti-inflammatory and antioxidant activity, improvement in mitochondrial function, and the inhibition of apoptosis, are all considered potential effects of resveratrol (Rauf et al., 2017).

Recently, grape seed has shown a potential for production of oil, up to 15%, as a by-product of winemaking (Teixeira et al., 2014). According to the Global GSO market 2019, indicates that the GSO production is expected to grow at a roughly 3.7% over the next five years, will reach 450 million US$ in 2024, from 360 million US$ in 2019. The global aim of the project is to assess whether resveratrol-enriched GSO, compared to other saturated fatty acid (SFA)-enriched high-fat diet (HFD), could have benefits on markers of metabolic abnormalities and inflammation in white adipose tissue of obese mice.

2. Materials and methods

2.1. Animals and diets

All animal protocols received appropriate institutional approval by Animal Care and Use Committee of the University Hospital Virgen Macarena and University Hospital Virgen del Rocio, and were performed according to the official rules formulated in the Spanish law and European legislation on the care and use of experimental animals (RD 53/2013; 2012/707/UE). C57BL/6J genetic background were used for this study. Mice were maintained in light/dark- (12 h light/12 h dark), temperature- (22 ± 1 °C) and humidity- (50–60% relative humidity) controlled room, fed with standard chow diet (CD, SAFE A04-10 Panlab) ad libitum and had free access to drinking water at the animal facilities of the School of Medicine (University of Seville).

Male animals at the age of 10–12 weeks were divided in 4 experimental groups (n = 10/group). Mice were fed chow diet (3% energy as fat from soybean oil, A04-10) or high-fat diets (HFDs) based on the above A04-10 diet with additional 21% energy as fat from milk cream (HFD-SFAs), or GSO (Naturgreen, Murcia, Spain) for 12 weeks. In one dietary GSO group, resveratrol (Sigma-aldrich, Madrid, Spain) was added in 200 mg/kg/day (Table 1) (Ding et al., 2018). Diets and drinking water were refreshed every week. The fatty acid composition of the diets was determined via lipid extraction, saponification and capillary gas chromatography (Table 2) (Montserrat-de la Paz et al., 2016). Total phenolic content (TPC) in GSO was carried out using the method described by Martin et al. (Martin et al., 2019). The TPC in GSO was 73.09 ± 1.71 μg per gram of GSO. These results are in line with previous studies (Bail, Stuebiger, Krist, Unterweger, & Buchbauer, 2008). Carbohydrate was used to adjust the total energy content in LFD and HFDs (isocaloric diets, 3339 Kcal/Kg). All diets had low cholesterol (0.01%), were prepared by Panlab and presented as pellets to the animals. Body mass, food and water intake were recorded daily.

Table 1
Macronutrients composition of diets.

Macronutrients	CD	HFD	GSO	GSO + R
Fat (%)	3	24	24	24
Carbohydrate (%)	77.5	56.5	56.5	56.5
Protein (%)	19.5	19.5	19.5	19.5

Values are expressed as the percentage of energy derived from fat, carbohydrate or protein. Chow diet (CD), high-fat diet rich in saturated fatty acids (HFD), high-fat diet rich in grape seed oil (GSO), and high-fat diet rich in GSO plus resveratrol (GSO + R).

Table 2
Fatty acid composition of dietary fats for corresponding HFD.

	HFD	GSO	GSO + R
Fatty acid	g/100 g of fatty acid ± SD		
4:0, butyric	0.83 ± 0.09	–	–
6:0, caproic	0.25 ± 0.01	–	–
8:0, caprylic	0.61 ± 0.04	–	–
10:0, capric	2.47 ± 0.08	–	–
12:0, lauric	3.09 ± 0.24	–	–
14:0, myristic	10.87 ± 0.53	0.05 ± 0.01	0.05 ± 0.01
16:0, palmitic	35.54 ± 0.47	6.73 ± 0.35	6.76 ± 0.33
18:0, stearic	11.49 ± 0.43	3.84 ± 0.21	3.85 ± 0.23
Total-SFAs	63.46 ± 1.07 [a]	10.62 ± 0.89[b]	10.66 ± 0.86[b]
16:1(n-7), palmitoleic	3.60 ± 0.18	0.17 ± 0.08	0.16 ± 0.08
18:1(n-9), oleic	25.33 ± 0.41	14.76 ± 0.42	14.68 ± 0.46
Total-MUFAs	28.93 ± 1.48[b]	14.93 ± 1.22 [a]	14.84 ± 1.13 [a]
18:2(n-6), linoleic	4.27 ± 0.47	74.16 ± 0.53	74.23 ± 0.51
18:3(n-3), α-linolenic	0.39 ± 0.03	0.11 ± 0.07	0.11 ± 0.07
Total-PUFAs	4.66 ± 0.46[b]	74.27 ± 1.75 [a]	74.34 ± 1.66 [a]
Others	0.96 ± 0.24	0.18 ± 0.02	0.16 ± 0.02

The values are expressed as the mean ± SD (n = 3). An ANOVA followed by Tukey's post-hoc test was performed. Different superscript letters (a–c) denote that mean values in a row with different letters are significantly different ($p < 0.05$). High-fat diet rich in saturated fatty acids (HFD), high-fat diet rich in grape seed oil (GSO), and high-fat diet rich in GSO plus resveratrol (GSO + R).

At the end of the experiments, animals were sacrificed at the beginning of the light cycle and after 10-h of food deprivation, blood was collected by cardiac puncture and tissues (WAT and interscapular brown adipose tissue, iBAT) were then removed, weighed, and frozen at −80 °C or fixed with 4% paraformaldehyde for further analysis.

2.2. Metabolic profiling

The oral glucose tolerance test (OGTT) was performed at least one week before sacrifice. For OGTT, mice were fasted overnight followed by oral gavage of dextrose (2 g/kg of body weight). Glucose was measured from tail vein blood at baseline and at 15, 30, 60, 90 and 120 min. At the time of sacrifice, fasting serum samples were used to measure cytokine and adipokine (TNF-α, IL-1β, IL-6, and leptin) levels by ELISA (ThermoFisher Scientific, Whaltham, MA, USA). Cholesterol and triglycerides in serum were determined by enzymatic colorimetric assays (Cholesterol Reagent and Triglycerides reagent kits from Bio-Science-Medical, Madrid, Spain).

2.3. Histological analysis

WAT tissue samples (5–10 mm) fixed in 4% paraformaldehyde were dehydrated in ethanol and xylene, and embedded in paraffin. The paraffin blocks were sliced into 6 μm tissue sections that were deparaffinized, rehydrated and stained for hematoxylin-eosin or macrophage immunohistochemistry. In the hematoxylin-eosin study, a standard Mayer's Hematoxylin and Eosin Y (H&E) staining protocol was used. Images were acquired using a Leica DM3000 light microscopy (Leica

Microsystems) coupled to a computerized morphometric system (Leica Qwin 3.5.1). Adipocyte area and size distribution were measured using ImageJ software. Adipocyte number was determined as described previously (Arner et al., 2013). Data were collected from 3 H&E-stained sections per mouse. Average of 100 cells per mouse is presented.

2.4. RNA isolation and RT-qPCR analysis

Total RNA was extracted from WAT and BAT samples using Trisure Reagent (Bioline, London, UK). RNA quality was assessed by A_{260}/A_{280} ratio in a NanoDrop ND-1000 Spectrophotometer (Thermo Scientific). RNA (1 μg) was subjected to reverse transcription (iScript, BioRad, Hercules, CA, USA). An amount of 20 ng of the resulting cDNA was used as a template for real-time PCR amplifications. The mRNA levels for specific genes were determined in a CFX96 system (BioRad). For each PCR reaction, cDNA template was added to Brilliant SYBR green QPCR Supermix (BioRad) containing the primer pairs for the corresponding gene. Glyceraldehyde 3-phosphate dehydrogenase (GAPDH) was used as housekeeping gene. Primers are available in Supplementary Table 1. All amplification reactions were performed in triplicate and average threshold cycle (Ct) numbers of the triplicates were used to calculate the relative mRNA expression of candidate genes. The magnitude of change of mRNA expression for candidate genes was calculated by using the standard $2^{-(\Delta\Delta Ct)}$ method. All data were normalized to the content of housekeeping gene and expressed as percentage of control.

2.5. Isolation and immunoblotting detection of proteins

BAT was processed as described by Aparicio-Soto *et al.* (Aparicio-Soto et al., 2018). Protein concentration was measured for each sample using a protein assay reagent (BioRad) according to the Bradfordś method using γ-globulin as a standard (Bradford, 1976). Aliquots of supernatant containing equal amount of proteins (20 μg) were separated on 10% acrylamide gel by sodium dodecyl sulphate polyacrylamide gel electrophoresis and the proteins were electrophoretically transferred into a nitrocellulose membrane and incubated with specific primary antibodies: polyclonal rabbit anti-mouse uncoupling protein one (UCP-1) (Cell Signaling, Danvers, MA, USA) and monoclonal rabbit anti-mouse β-actin (Sigma-Aldrich) antibodies; overnight at 4 °C. After rinsing, the membranes were incubated with a horseradish peroxidase-labelled (HRP) secondary antibody anti-rabbit (Cayman Chemical) (1:50,000) containing blocking solution for 1–2 h at room temperature. Immunodetection was performed using enhanced chemiluminescence light-detecting kit (Pierce, Rockford, IL, USA). The signals were captured using LAS-3000 Imaging System from Fujifilm Image Reader (Stamford, USA) and densitometry data were studied following normalization to the housekeeping loading control. The signals were analysed and quantified by an Image Processing and Analysis in Java (Image J, Softonic, Barcelona, Spain) and expressed in relation to CD group.

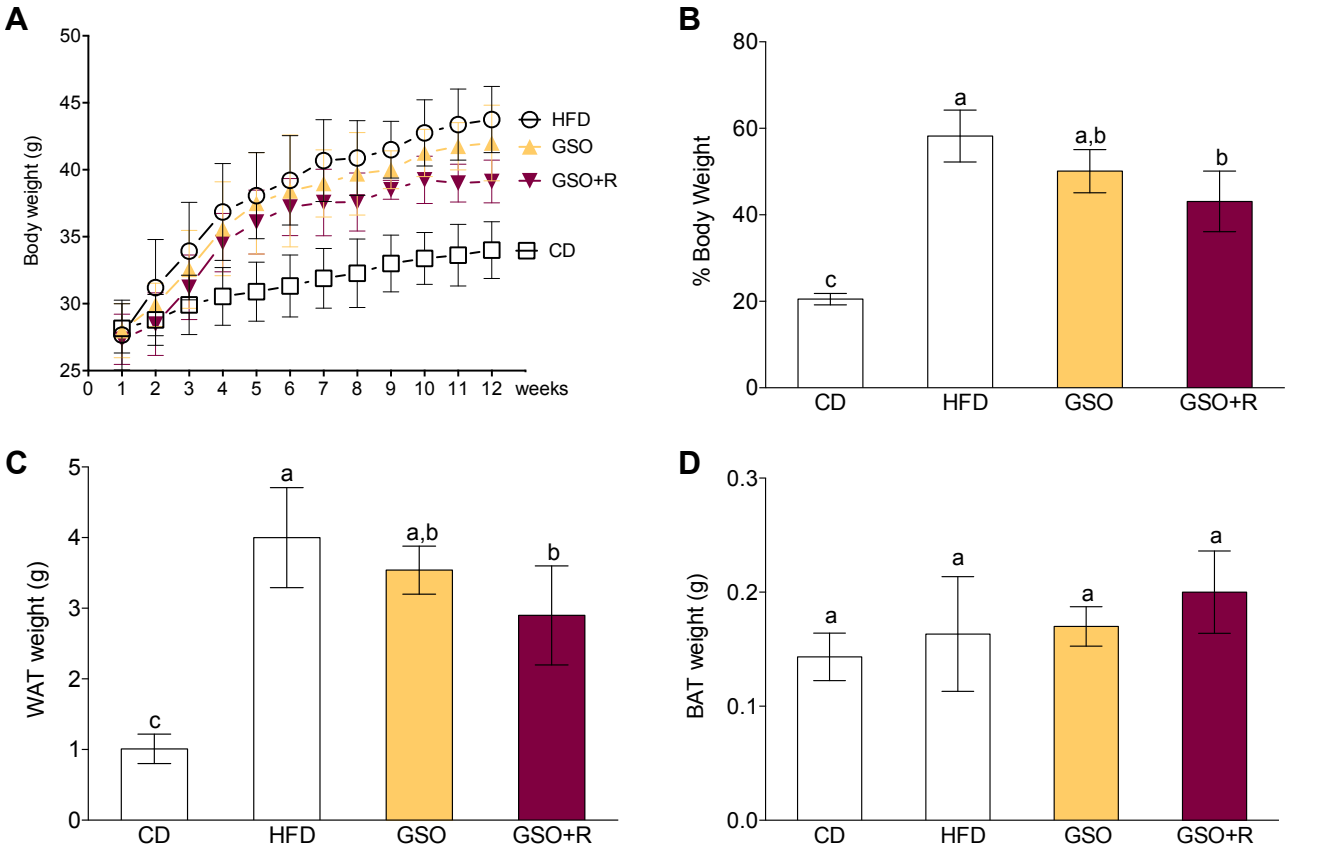

Fig. 1. Body weight monitored over time on each diet (A), body weight gain (B), WAT (C) and BAT (D) weight after 12 weeks feeding on each diet (n = 10/diet). Values are presented as the mean ± SD and those marked with different lowercase letter are statistically different ($p < 0.05$).

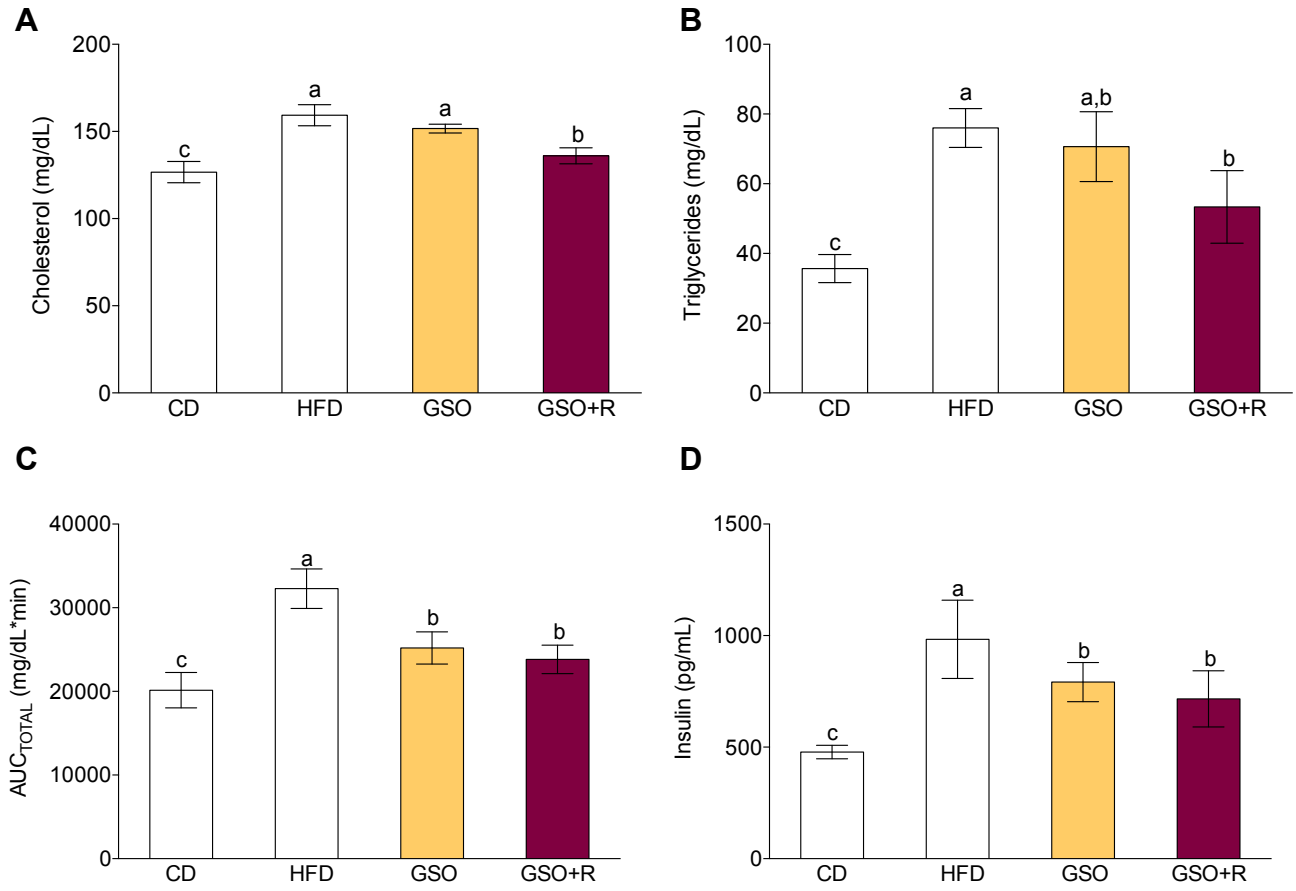

Fig. 2. Serum cholesterol (A), triglycerides (B), OGTT area-under-the-curve (C), and serum insulin (D) after 12 weeks feeding on each diet (n = 10/diet). Values are presented as the mean ± SD and those marked with different lowercase letter are statistically different ($p < 0.05$).

2.6. Statistical analysis

Data are presented as mean ± SD. Differences between groups were evaluated using one-way analysis of variance (ANOVA). Variables over time were evaluated with two-way ANOVA with Tukey multiple comparisons post-hoc. GraphPad Prism version 7 was used for these statistical analyses. Criterion for significance was set to $p < 0.05$ in all comparisons.

3. Results

3.1. Resveratrol-enriched grape seed oil reduces body and white adipose tissue weight gain in obese mice

After 12 weeks of treatment, mean daily food intake (CD, 4.18 ± 0.27; HFD, 4.16 ± 0.72; GSO, 4.11 ± 0.35; GSO + R, 4.09 ± 0.48 g/mouse) and water intake (CD, 5.88 ± 0.97; HFD, 6.00 ± 1.03; GSO, 5.97 ± 0.79; GSO + R, 5.99 ± 0.96 mL/mouse) were not different among the four diet groups. Despite similarities in food and drink intake, the final body weight (Fig. 1A) and body weight gain (Fig. 1B) of animals increased but to a different degree depending on the diet (HFD > GSO > GSO + R > CD). WAT weights were significantly higher in mice on HFDs relative to chow diet but the effects of GSO + R were less pronounced than that of SFA-enriched HFD (Fig. 1C). No changes were observed for weight of iBAT (Fig. 1D), even when viewed from a weight-adjusted approach (data not shown).

3.2. Resveratrol-enriched grape seed oil attenuates lipid metabolism abnormalities and insulin resistance in obese mice

As obesity is associated with abnormal lipid metabolism, we next investigated parameters related to lipid metabolism in obese mice fed chow diet and HFDs. Serum cholesterol (Fig. 2A) and triglyceride (Fig. 2B) levels were significantly higher in mice on HFDs, although circulating cholesterol and triglycerides were lower in mice fed GSO + R as compared to SFA-enriched HFD. To establish if the impact of HFDs on body weight had consequences on glucose homeostasis, we assessed glycemic control in mice fed chow diet and HFDs. Mice fed GSO and GSO + R demonstrated better oral glucose tolerance (Fig. 2C) than mice fed SFA-enriched mice. Fasting blood glucose levels were comparable in all animals irrespective of diet (data not shown) but those on HFDs had higher fasting serum insulin levels (Fig. 2D) than the group on chow diet. Remarkably, impaired glucose homeostasis became less prominent with GSO and GSO + R than with SFA-enriched HFD.

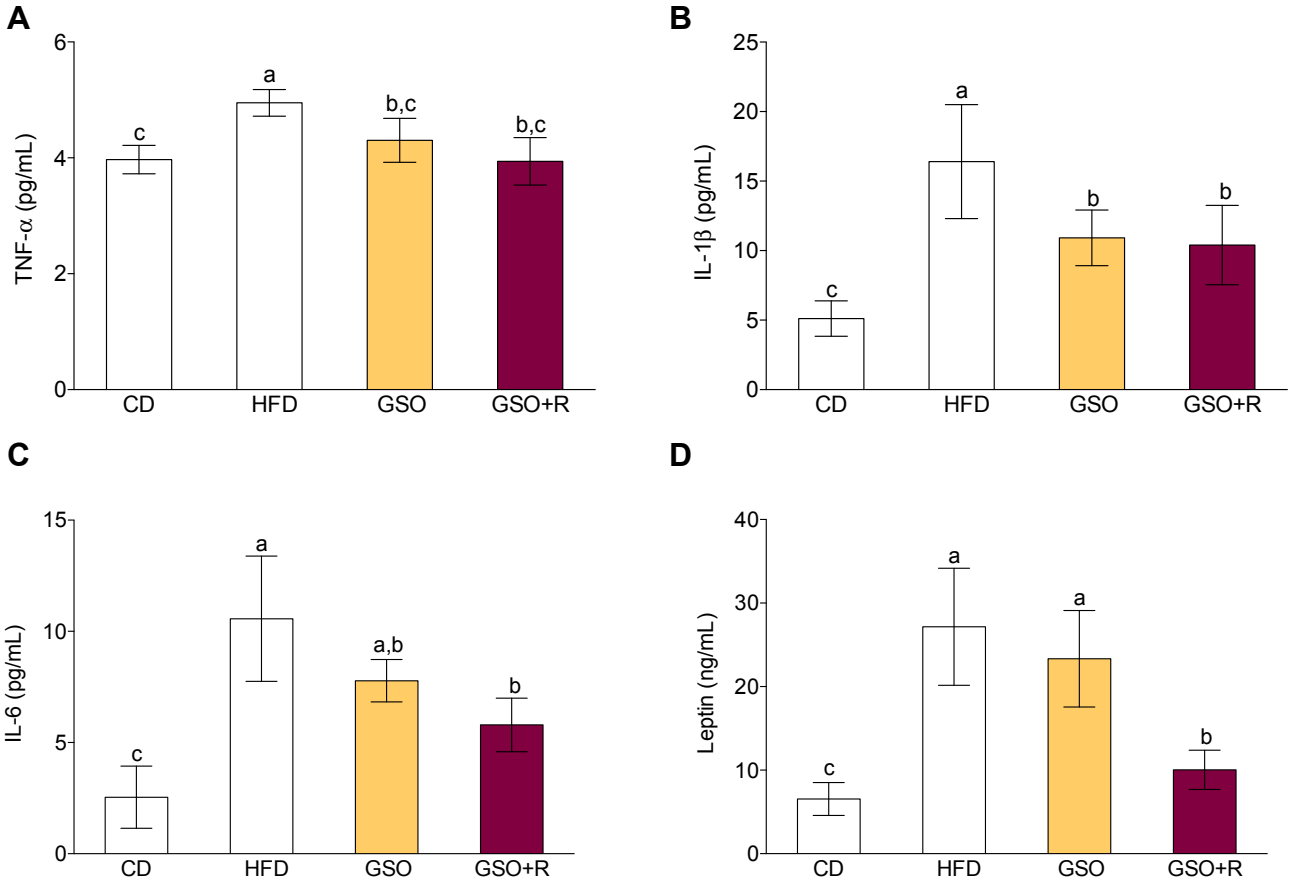

Fig. 3. Serum TNF-α (A), IL-1β (B), IL-6 (C), and leptin (D) after 12 weeks feeding on each diet (n = 10/diet). Values are presented as the mean ± SD and those marked with different lowercase letter are statistically different ($p < 0.05$).

3.3. Resveratrol-enriched grape seed oil improves low-grade systemic inflammation in obese mice

To gain understanding of the impact of HFDs on adipose tissue function and as obesity triggers chronic low-grade inflammation, we sought to determine the abundance of major circulating pro-inflammatory adipokines in mice fed chow diet and HFDs. As shown in Fig. 3, serum TNF-α (Fig. 3A), IL-1β (Fig. 3B), IL-6 (Fig. 3C), and leptin (Fig. 3D) levels were substantially higher in mice on SFA-enriched HFD. Interestingly, mice fed GSO + R showed less metabolically pro-inflammatory phenotype than mice fed SFA-enriched HFD.

3.4. Resveratrol-enriched grape seed oil attenuates white adipose tissue expansion in obese mice

Next, we performed studies to elucidate the adipocyte-architecture during adipose expansion in mice fed chow diet and HFDs. Histological examination of WAT sections (Fig. 4A) and subsequent quantification for adipocyte size confirmed a higher frequency of very large adipocytes (Fig. 4B) in mice fed HFDs. Noteworthy, mice fed GSO + R exhibited much less adipose hypertrophy (Fig. 4C) than mice fed SFA-enriched HFD and partially restored the adipocyte number compared to mice fed chow diet (Fig. 4D).

3.5. Resveratrol-enriched grape seed oil attenuates white adipose tissue infiltration and inflammation in obese mice

To explore immune-related events that follow adipose tissue expansion and that contribute to the development of insulin resistance, we analyzed the cellularity and recruitment of inflammatory cells and local inflammation in WAT of mice fed chow diet and HFDs. Upon mRNA levels for the pan macrophage marker F4/80 (Fig. 5A), the M1 macrophage marker CCR7 and iNOS (Fig. 5(B and C), respectively) and the M2 macrophage marker MRC-1 and Arg-1 (Fig. 5(D and E), respectively), we found that SFA-enriched HFD resulted in a dramatic increase of macrophages mainly polarized toward a M1 pro-inflammatory phenotype while GSO and GSO + R induced a much less infiltration of macrophages, the majority of which were M2. In addition, adipose gene expression levels of pro-inflammatory adipokines TNF-α (Fig. 6A), IL-1β (Fig. 6B), and IL-6 (Fig. 6C) were higher with SFA-enriched HFD but these levels were significantly down-regulated by GSO and GSO + R.

3.6. Resveratrol-enriched grape seed oil induces UCP-1 gene and protein expression in brown adipose tissue

Finally, the UCP-1 gene (Fig. 7A) and protein (Fig. 7B) expression

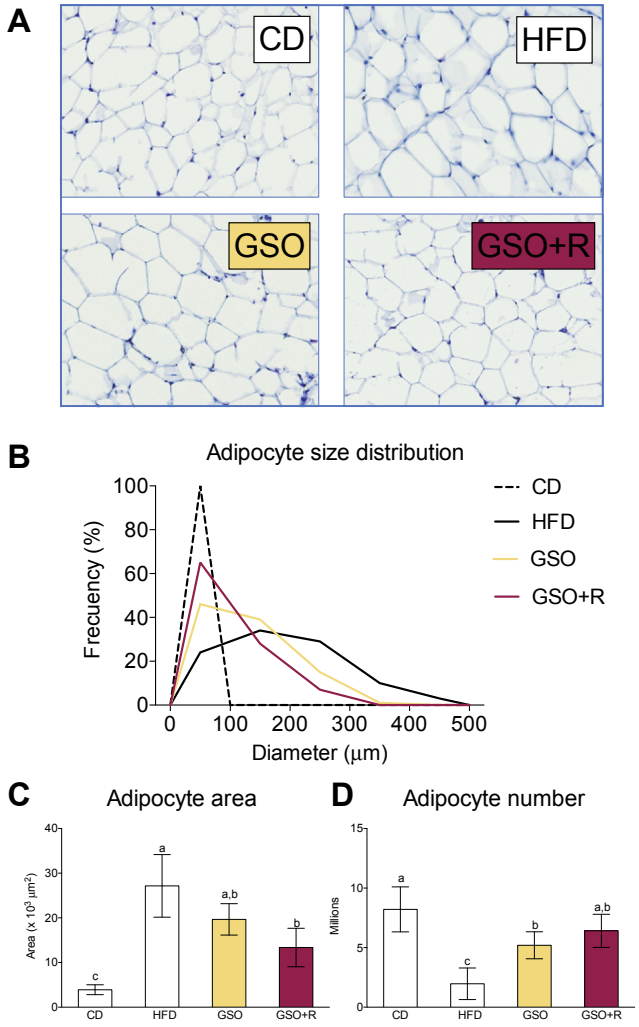

Fig. 4. Representative H&E stained histological sections (A), frequency of adipocyte cell surface area (B), mean adipocyte size (C), and mean adipocyte number (D) after 12 weeks feeding on each diet (n = 10/diet). Values are presented as the mean ± SD and those marked with different lowercase letter are statistically different ($p < 0.05$).

levels were analyzed in BAT of mice fed chow diet and HFDs. No differences were observed between SFA-enriched HFD and chow diet, whereas GSO + R significantly increased mRNA and protein levels in BAT.

4. Discussion

The interest in grapes as a functional food product has increased, especially because of its high levels of bioactive constituents in wine-making by-products, such as resveratrol in skins and lipophilic constituents, such as vitamin E, unsaturated fatty acids, and phytosterols in GSO (Karaman et al., 2015). Despite the potential health benefits of resveratrol, its utilization as a nutraceutical ingredient within the food industry is currently limited due to its poor water-solubility, chemical instability, and low bioavailability (Davidov-Pardo & McClements, 2015) In the present work, the GSO has been enriched in resveratrol and for the first time, the effect of this functional food has been explored on metabolic and inflammatory response of WAT from obese mice. Our study further demonstrated that dietary resveratrol-enriched GSO could reverse insulin resistance and lipid abnormalities, reduce low-grade systemic inflammation, and decrease WAT expansion, immune cell infiltration and inflammation in HFD-induced obese mice.

To our knowledge, for the first time, these effects of dietary GSO have been demonstrated in HFD-induced obese mice. However, studies in animal models of diabetes and obesity have shown that resveratrol mitigates complications of metabolic diseases (Carpéné et al., 2019). In rodents, the range of doses used in the reported studies with resveratrol is very large (1–400 mg/kg body weight/day). This means that resveratrol shows anti-obesity effects at doses clearly below the no observed adverse effect level (NOAEL), fixed at 750 mg/kg/day. By extrapolating these doses to humans using Reagan-Shaw's formula (Reagan-Shaw, Nihal, & Ahmad, 2008), the doses obtained are in the range of 0.081–10.8 mg/kg/day, which represents 4.9–648 mg/day for a 60-kg adult (Edwards, Beck, Riegger, & Bausch, 2011).

Our approach did not allow for deciphering the exact mechanisms by which resveratrol (200 mg/Kg/day)-enriched GSO prevents fat accumulation in treated obese mice. However, as expected, the main target for resveratrol as an anti-obesity molecule is WAT, because it is the main body lipid store. Accordingly, we observed body and WAT weight gain and serum lipid concentration were significantly lower in mice on resveratrol-enriched GSO relative to SFA-enriched HFD. In this sense, previous investigations demonstrated a significant reduction induced by resveratrol in serum TG and TC levels in animal models of obesity, accompanied by reduced body weight gain (Liu et al., 2016; Qiao et al., 2014; Rivera, Moron, Zarzuelo, & Galisteo, 2009). Consequently, the mechanism of resveratrol by regulating lipid abnormalities in obesity is not totally understood and needs further research.

In obesity, the hypertrophy and hyperplasia or both become dysfunctional WAT. Resveratrol-enriched GSO undergoes healthy expansion if the HFD is mainly composed by GSO instead of SFAs. In addition, macrophage infiltration into adipose tissues is characteristic of chronic inflammation associated with obesity and a low-grade systemic inflammation. Recently, macrophage polarization has been proposed to be attractive targets for anti-obesity. Increasing evidence has shown that M1 macrophage recruitment and infiltration into WAT promote the pathogenesis of insulin resistance (Huh et al., 2017). Thus, we studied the effect of resveratrol-enriched GSO in macrophage content into WAT during the development of obesity. Consistent with the increased expression of serum inflammatory adipokines (such as TNF-α, IL-1β, IL-6, and leptin) in obese mice, we demonstrated that the content and M1 marker expression in WAT were significantly increased in SFA-enriched HFD compared to chow diet. Resveratrol-enriched GSO partially restored WAT healthy status of WAT. *In vitro*, resveratrol inhibited the mRNA and protein expression of M1 marker in THP-1 monocytes (Cullen et al., 2007).

In addition to WAT, BAT is also a target for resveratrol. The main role of BAT is not fat accumulation but adaptive thermogenesis, which is defined as heat production in response to environmental temperature or diet (Lowell & Spiegelman, 2000). It is mediated by UCP1, located in the inner mitochondrial membrane. UCP1 can dissipate surplus caloric energy and consequently be an important regulator of body weight. As a matter of fact, BAT may prevent obesity by allowing combustion of energy instead of storing the excess energy as fat (Cannon &

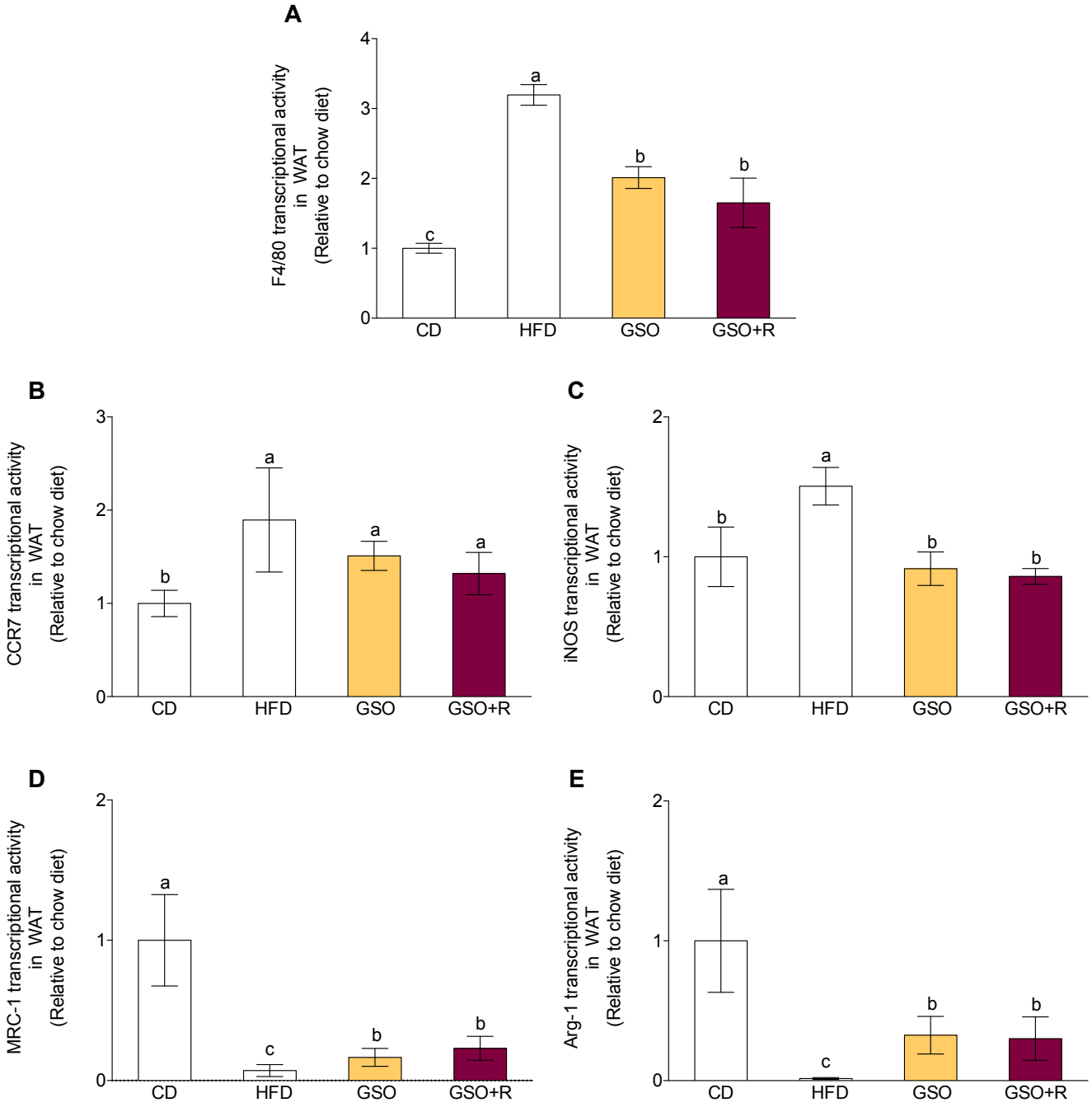

Fig. 5. Relative gene expression in WAT by RT-qPCR of F4/80 (A), CCR7 (B), iNOS (C), MRC-1 (D), and Arg-1 (E) after 12 weeks feeding on each diet (n = 10/diet). Values are presented as the mean ± SD and those marked with different lowercase letter are statistically different ($p < 0.05$).

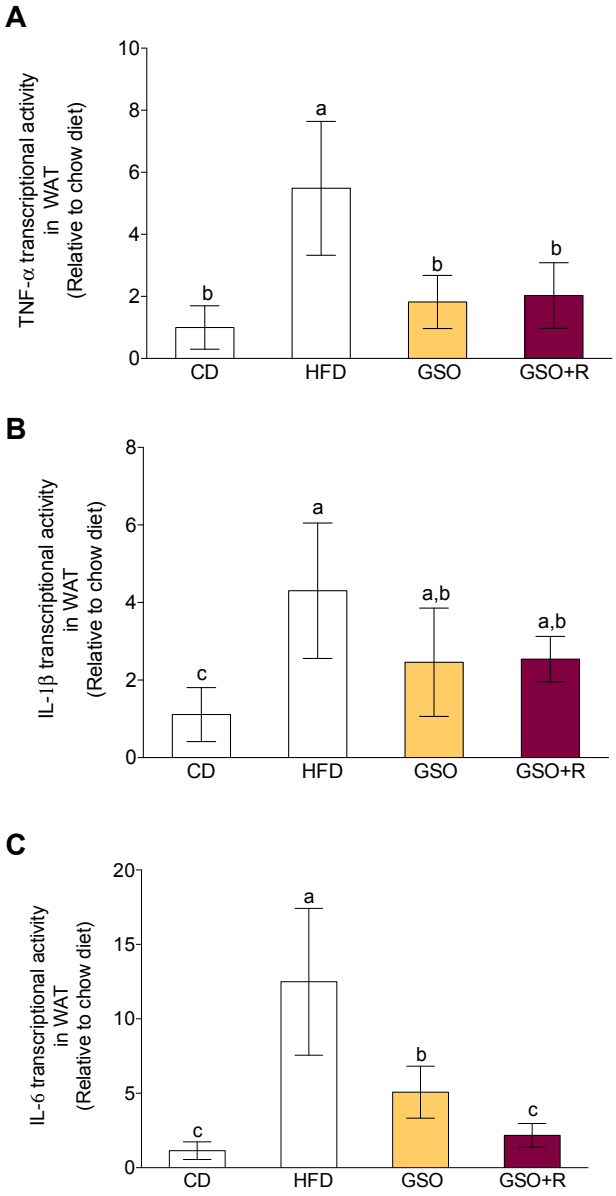

Fig. 6. Relative gene expression in WAT by RT-qPCR of TNF-α (A), IL-1β (B), and IL-6 (C) after 12 weeks feeding on each diet (n = 10/diet). Values are presented as the mean ± SD and those marked with different lowercase letter are statistically different ($p < 0.05$).

Nedergaard, 2012). Recently, Wang et al. (2017) observed a decrease in the average daily weight gain and morphological changes in interscapular BAT (iBAT) in mice treated with resveratrol (0.1% w/w in an HFD) for 4 weeks. Furthermore, the authors observed an increase in UCP1 gene and protein expression in the resveratrol-supplemented animal.

5. Conclusion

Herein, we demonstrated for the first time that concomitant with a decrease in M1 marker expression and total macrophage F4/80 in WAT, proinflammatory adipokines in serum, and mRNA levels of inflammatory adipokines in WAT were significantly reduced and UCP1 gene and protein expression in BAT was significantly increased in resveratrol-enriched GSO obese mice (Fig. 8). This study unveils new beneficial effects of the combination of two winemaking by-products and establishes the potential use of this resveratrol-enriched grape seed oil in the prevention of obesity and its comorbidities.

Ethics statements file

This study was conducted according to Good Clinical Practice Guidelines and in line with the principles outlined in the Helsinki Declaration of the World Medical Association. Informed consent for the study was obtained. All animal protocols received appropriate institutional approval (Animal Care and Use Committee of the University of Seville) and were performed according to the official rules formulated in the Spanish law on the care and use of experimental animals (UE Directive of 2010: 2010/63/UE; RD 53/2013).

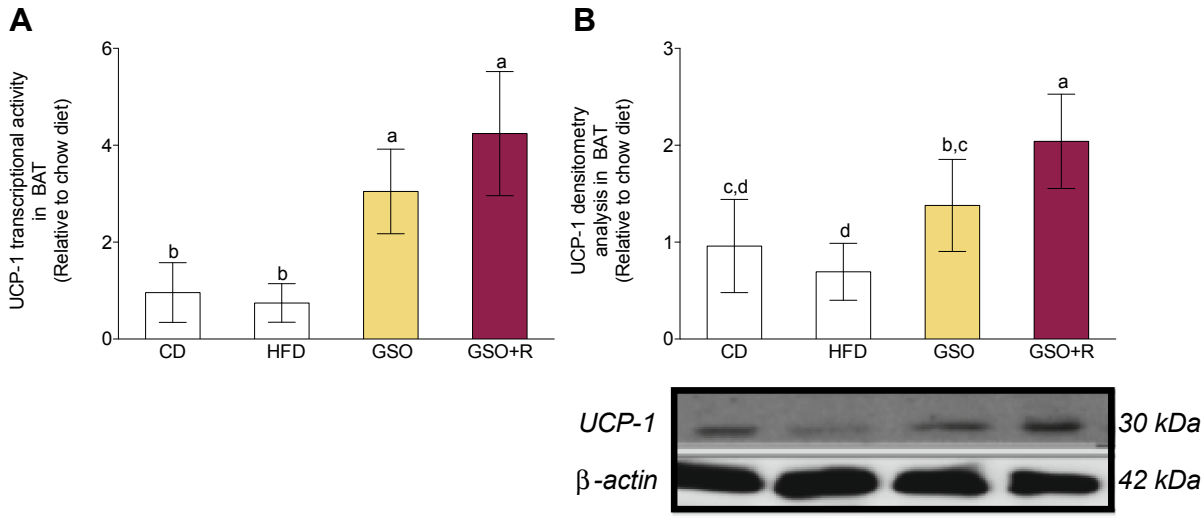

Fig. 7. Relative gene expression (A) and protein expression (B) in BAT of UCP-1 after 12 weeks feeding on each diet (n = 10/diet). Values are presented as the mean ± SD and those marked with different lowercase letter are statistically different ($p < 0.05$).

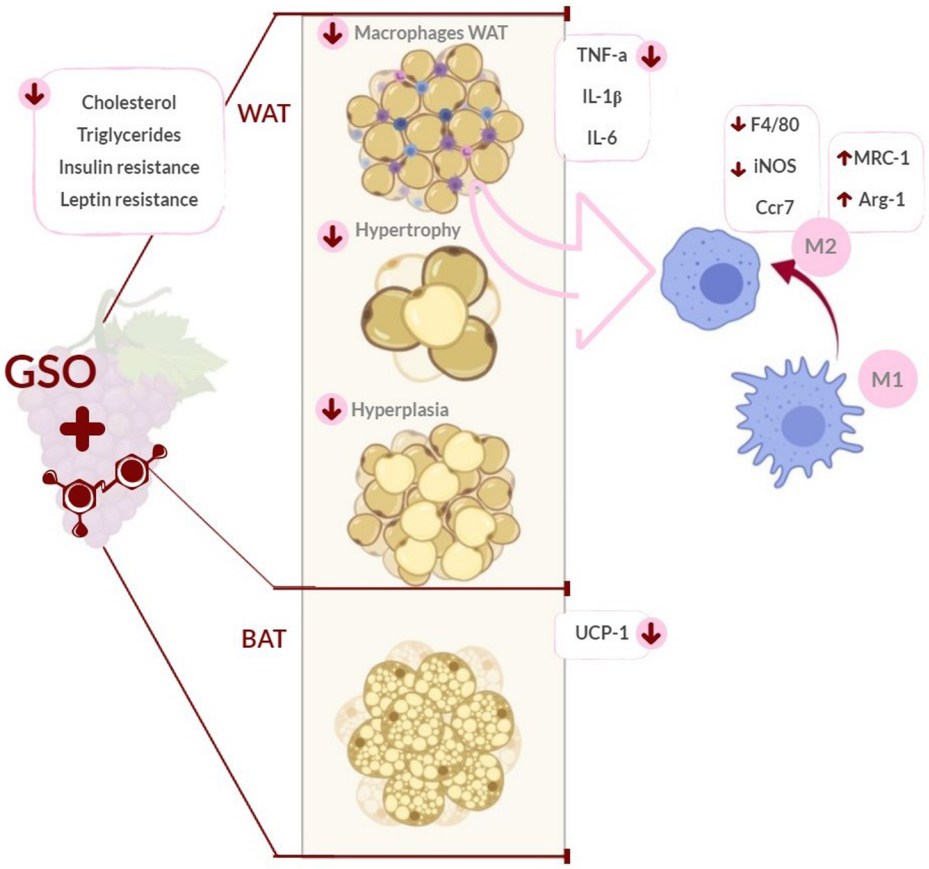

Fig. 8. Summary of metabolic effects in WAT and BAT after 12 weeks feeding on HFD containing resveratrol-enriched GSO.

Declaration of Competing Interest

The authors state no conflict of interest.

Acknowledgements

Authors thank Cell Biology Unit of Instituto de la Grasa for its assistance during the fulfilment of this work. SMP acknowledges financial support from "V Own Research Plan" (University of Seville).

Appendix A. Supplementary material

Supplementary data to this article can be found online at https://doi.org/10.1016/j.jff.2019.103546.

References

Aguirre, L., Fernandez-Quintela, A., Arias, N., & Portillo, M. P. (2014). Resveratrol: Anti-obesity mechanisms of action. *Molecules, 19*, 18632–18655.

Aparicio-Soto, M., Montserrat-de la Paz, S., Sanchez-Hidalgo, M., Cardeno, A., Bermudez, B., Muriana, F. J. G., & Alarcon-de-la-Lastra, C. (2018). Virgin olive oil and its phenol fraction modulate monocyte/macrophage functionality: A potential therapeutic strategy in the treatment of systemic lupus erythematosus. *British Journal of Nutrition, 120*, 681–692.

Arner, P., Andersson, D. P., Thörne, A., Wirén, M., Hoffstedt, J., Näslund, E., ... Rydén, M. (2013). Variations in the size of the major omentum are primarily determined by fat cell number. *Journal of Clinical Endocrinology & Metabolism, 98*, E897–E901.

Bail, S., Stuebiger, G., Krist, S., Unterweger, H., & Buchbauer, G. (2008). Characterisation of various grape seed oils by volatile compounds, triacylglycerol composition, total phenols and antioxidant capacity. *Food Chemistry, 108*, 1122–1132.

Bonnefont-Rousselot, D. (2016). Resveratrol and cardiovascular diseases. *Nutrients, 8*, E250.

Bradford, M. M. (1976). A rapid and sensitive method for the quantitation of microgram quantities of protein utilizing the principle of protein-dye binding. *Analytical Biochemistry, 72*, 248–254.

Cannon, B., & Nedergaard, J. (2012). Cell biology: Neither brown nor white. *Nature, 488*, 286–287.

Carpéné, C., Les, F., Cásedas, G., Peiro, C., Fontaine, J., Chaplin, A., ... López, V. (2019). Resveratrol anti-obesity effects: Rapid inhibition of adipocyte glucose utilization. *Antioxidants, 8*, 74.

Choe, S. S., Huh, J. Y., Hwang, I. J., Kim, J. I., & Kim, J. B. (2016). Adipose tissue remodeling: Its role in energy metabolism and metabolic disorders. *Frontiers in Endocrinology, 7*, 30.

Cullen, J. P., Morrow, D., Jin, Y., von Offenberg Sweeney, N., Sitzmann, J. V., Cahill, P. A., & Redmond, E. M. (2007). Resveratrol inhibits expression and binding activity of the monocyte chemotactic protein-1 receptor, CCR2, on THP-1 monocytes. *Atherosclerosis, 195*, e125–e133.

Davidov-Pardo, G., & McClements, D. J. (2015). Nutraceutical delivery systems: Resveratrol encapsulation in grape seed oil nanoemulsions formed by spontaneous emulsification. *Food Chemistry, 167*, 205–212.

Diaz, M., Degens, H., Vanhees, L., Austin, C., & Azzawi, M. (2016). The effects of resveratrol on aging vessels. *Experimental Gerontology, 85*, 41–47.

Ding, S., Jiang, J., Wang, Z., Zhang, G., Yin, J., Wang, X., ... Yu, Z. (2018). Resveratrol reduces the inflammatory response in adipose tissue and improves adipose insulin signaling in high-fat diet-fed mice. *PeerJ, 6*, e5173.

Edwards, J. A., Beck, M., Riegger, C., & Bausch, J. (2011). Safety of resveratrol with examples for high purity, trans-resveratrol, resVidaR. *Annals of the New York Academy of Sciences, 1215*, 131–137.

Gonzalez-Muniesa, P., Martinez-Gonzalez, M. A., Hu, P. B., Despres, J. P., Matsuzawa, Y., Loos, R. J. F., ... Martinez, J. A. (2017). Obesity. *Nature Reviews Disease Primers, 3*, 17034.

Guo, F., He, H., Fu, Z. C., Huang, S., Chen, T., Papasian, C. J., ... Fu, M. (2015). Adipocyte-derived PAMM suppresses macrophage inflammation by inhibiting MAPK signaling. *Biochemical Journal, 472*, 309–318.

Huh, J. H., Kim, H. M., Lee, E. S., Kwon, M. H., Lee, B. R., Ko, H. J., & Chung, C. H. (2017). Dual CCR2/5 antagonist attenuates obesity-induced insulin resistance by regulating macrophage recruitment and M1/M2 status. *Obesity, 26*, 378–386.

Karaman, S., Karasu, S., Tornuk, F., Toker, O. S., Gecgel, U., Sagdic, O., ... Gul, O. (2015). Recovery potential of cold press byproduct obtained from the edible oil industry: Physicochemical, bioactive, and microbial properties. *Journal of Agricultural & Food Chemistry, 63*, 2305–2313.

Ko, J. H., Sethi, G., Um, J. Y., Shanmugam, M. K., Arfuso, F., Kumar, A. P., ... Ahn, K. S. (2017). The role of resveratrol in cancer therapy. *International Journal of Molecular Science, 18*, E2589.

Liu, Z., Gan, L., Liu, G., Chen, Y., Wu, T., Feng, F., & Sun, C. (2016). Sirt1 decreased adipose inflammation by interacting with Akt2 and inhibiting mTOR/S6K1 pathway in mice. *Journal of Lipid Research, 57*, 1373–1381.

Lowell, B. B., & Spiegelman, B. M. (2000). Towards a molecular understanding of adaptive thermogenesis. *Nature, 404*, 652–660.

Macdougall, C. E., & Longhi, M. P. (2019). Adipose tissue dendritic cells in steady-state. *Immunology, 156*, 228–234.

Martin, M. E., Millan-Linares, M. C., Naranjo, M. C., Toscano, R., Abia, R., Muriana, F. J. G., ... Montserrat-de la Paz, S. (2019). Minor compounds from virgin olive oil attenuate LPS-induced inflammation via visfatin-related gene modulation on primary human monocytes. *Journal of Food Biochemistry, 43*, e12941.

Millan-Linares, M. C., Bermudez, B., Martin, M. E., Muñoz, E., Abia, R., Millan, F., ... Montserrat-de la Paz, S. (2018). Unsaponifiable fraction isolated from grape (*Vitis vinifera* L.) seed oil attenuates oxidative and inflammatory responses in human primary monocytes. *Food & Function, 9*, 2517–2523.

Montserrat-de la Paz, S., Naranjo, M. C., Lopez, S., Abia, R., Muriana, F. J. G., & Bermudez, B. (2016). Olive oil, compared to a saturated dietary fat, has a protective role on atherosclerosis in niacin-treated mice with metabolic syndrome. *Journal of Functional Foods, 26*, 557–564.

Qiao, Y., Sun, J., Xia, S., Tang, X., Shi, Y., & Le, G. (2014). Effects of resveratrol on gut microbiota and fat storage in a mouse model with high-fat-induced obesity. *Food & Function, 5*, 1241–1249.

Rauf, A., Imran, M., Suleria, H. A. R., Ahmad, B., Peters, D. G., & Mubarak, M. S. (2017). A comprehensive review of the health perspectives of resveratrol. *Food & Function, 8*, 4284–4305.

Reagan-Shaw, S., Nihal, M., & Ahmad, N. (2008). Dose translation from animal to human studies revisited. *FASEB Journal, 22*, 659–661.

Rivera, L., Moron, R., Zarzuelo, A., & Galisteo, M. (2009). Long-term resveratrol administration reduces metabolic disturbances and lowers blood pressure in obese Zucker rats. *Biochemical Pharmacology, 77*, 1053–1063.

Stelmach-Mardas, M., Rodacki, T., Dobrowolska-Iwanek, J., Brzozowska, A., Walkowiak, J., Wojtanowska-Krosniak, A., ... Boeing, H. (2016). Link between food energy density and body weight changes in obese adults. *Nutrients, 8*, 229.

Szkudelski, T., & Szkudelska, K. (2015). Resveratrol and diabetes: From animal to human studies. *Biochimica et Biophysica Acta, 1852*, 1145–1154.

Teixeira, A., Baenas, N., Dominguez-Perles, R., Barros, A., Rosa, E., Moreno, D. A., & Garcia-Viguera, C. (2014). Natural bioactive compounds from winery by-products as health promoters: A review. *International Journal of Molecular Sciences, 15*, 15638–15678.

Wang, S., Liang, X., Yang, Q., Fu, X., Zhu, M., Rodgers, B. D., ... Du, M. (2017). Resveratrol enhances brown adipocyte formation and function by activating AMP-activated protein kinase (AMPK) alpha1 in mice fed high-fat diet. *Molecular Nutrition & Food Research, 61*, 1600746.

Yang, X., Xu, S., Qian, Y., & Xiao, Q. (2017). Resveratrol regulates microglia M1/M2 polarization via PGC-1a in conditions of neuroinflammatory injury. *Brain, Behavior, and Immunity, 64*, 162–172.

Zhao, H., Shang, Q., Pan, Z., Bai, Y., Li, Z., Zhang, H., ... Wang, Q. (2018). Exosomes from adipose-derived stem cells attenuate adipose inflammation and obesity through polarizing M2 macrophages and beiging in white adipose tissue. *Diabetes, 67*, 235–247.